Click Here for Full Article

# Assessment of sprite initiating electric fields and quenching altitude of $a^1\Pi_g$ state of $N_2$ using sprite streamer modeling and ISUAL spectrophotometric measurements

Ningyu Liu,[1] Victor P. Pasko,[2] Harald U. Frey,[3] Stephen B. Mende,[3] Han-Tzong Su,[4] Alfred B. Chen,[4] Rue-Ron Hsu,[4] and Lou-Chuang Lee[5]

Received 6 September 2008; revised 4 December 2008; accepted 19 January 2009; published 26 March 2009.

[1] In this study, we compare sprite streamer modeling results with Imager of Sprites and Upper Atmospheric Lightning (ISUAL) spectrophotometric data for several sprite events. The model positive streamers are simulated for two representative magnitudes of the quasi-electrostatic field produced by cloud-to-ground lightning discharges, reflecting conditions at 70 km altitude during the initial stage of sprite formation. The intensity ratio of the second positive band system of $N_2$ ($2PN_2$) to the first negative system of $N_2^+$ ($1NN_2^+$) is obtained separately from the modeling and the ISUAL measurements. The comparison results indicate that the ratio obtained for the streamer developing in an electric field close to the conventional breakdown threshold field $E_k$ agrees with the ISUAL measurements at the very early stage of the sprite development better than for the streamer developing in a field much lower than $E_k$. This finding supports the sprite theory proposing that sprites are caused by conventional breakdown of air when the lightning field in the upper atmosphere exceeds the local breakdown threshold field, which has also been supported by a recent study by Hu et al. (2007) comparing modeled lightning fields obtained using measured current moments of causative lightning discharges and video observations of sprites. The fact that the early stage emissions from the sprites under study are well explained by the radiation from streamers in strong fields allows the use of ISUAL data to gain additional information on the poorly known quenching altitude of the $N_2(a^1\Pi_g)$ state, which is responsible for $N_2$ Lyman-Birge-Hopfield band system. The results confirm that the 77 km suggested in previous study by Liu and Pasko (2005) is a good estimate for the quenching altitude of $N_2(a^1\Pi_g)$.

**Citation:** Liu, N., V. P. Pasko, H. U. Frey, S. B. Mende, H.-T. Su, A. B. Chen, R.-R. Hsu, and L.-C. Lee (2009), Assessment of sprite initiating electric fields and quenching altitude of $a^1\Pi_g$ state of $N_2$ using sprite streamer modeling and ISUAL spectrophotometric measurements, *J. Geophys. Res.*, *114*, A00E02, doi:10.1029/2008JA013735.

## 1. Introduction

[2] Sprites are large luminous discharges, which appear in the altitude range of ~40 to 90 km above thunderstorms typically following intense positive cloud-to-ground (CG) lightning discharges [*Sentman et al.*, 1995; *Boccippio et al.*, 1995]. A review of the current knowledge on sprites emphasizing their molecular physics and similarity with laboratory discharges is given by *Pasko* [2007]. We briefly explain the occurrence of sprites below. After CG lightning discharges remove single polarity charge to the ground, an electric field temporarily appears above the thundercloud in the mesosphere/lower ionosphere. The strength of the field is generally proportional to the charge moment change due to the causative lightning discharge, and the persistence of the field in time is approximately determined by the local dielectric relaxation time in the conducting atmosphere [*Pasko et al.*, 1997; *Pasko*, 2007]. The altitude profile of the lightning induced field is similar to that of an electric dipole consisting of a monopole charge and its ground image. The magnitude of this field approximately depends on the altitude $r$ as a function of $1/r^3$. A more accurate description of this field should also include contributions of image charges in the ionosphere, which leads to infinite line of image charges under ground and above the ionosphere [see *Pasko et al.*, 1997]. We note that representative

[1]Geospace Physics Laboratory, Department of Physics and Space Sciences, Florida Institute of Technology, Melbourne, Florida, USA.
[2]Communications and Space Sciences Laboratory, Pennsylvania State University, University Park, Pennsylvania, USA.
[3]Space Sciences Laboratory, University of California, Berkeley, California, USA.
[4]Department of Physics, National Cheng Kung University, Tainan, Taiwan.
[5]Institute of Space Science, National Central University, Jhongli, Taiwan.

Copyright 2009 by the American Geophysical Union.
0148-0227/09/2008JA013735$09.00

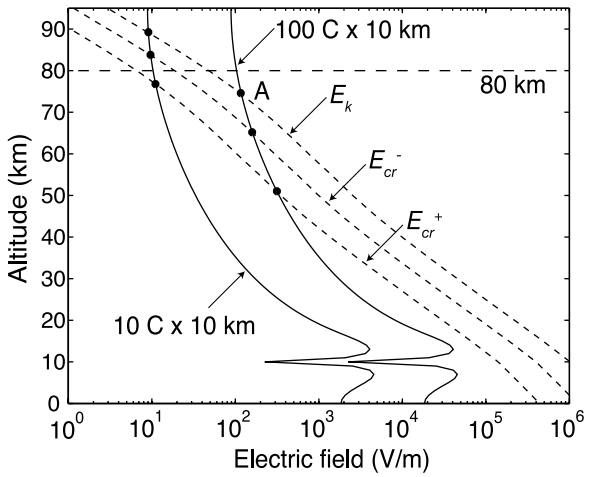


**Figure 1.** The altitude profiles of quasi-electrostatic fields produced by lightning, the conventional breakdown threshold field $E_k$, and the minimum fields required for stable propagation of streamers of positive ($E_{cr}^+$) and negative ($E_{cr}^-$) polarity.

field distributions illustrated in Figure 1 are obtained by exact numerical solution accounting for both ground and lower ionospheric conducting boundaries and related image charges. If we consider the dielectric strength of the Earth's atmosphere, we know the breakdown threshold field of air is proportional to the neutral density and thus exponentially decreases when altitude increases. It is possible that the lightning field exceeds the breakdown threshold field at mesospheric and lower ionospheric altitudes for a short period of time if the lightning removes a large amount of charge from a thundercloud. During this period, streamer type of air discharges is able to fully develop and produce the spectacular scene of sprites [*Pasko et al.*, 1998; *Liu and Pasko*, 2004]. A detailed, quantitative comparison between the sprite video observations and numerical simulations of electromagnetic fields produced by CG lightning discharges indicates that bright, short-delayed sprites are initiated when the lightning field reaches magnitudes exceeding 80% of the conventional breakdown threshold of air [*Hu et al.*, 2007]. The details how sprites/sprite streamers initiate when the lightning field is less than the threshold field are currently unknown. Two possible mechanisms have been proposed so far: (1) Sprite streamers are initiated at the bottom of the sprite halos, where the large ionization and electric field enhancements provide favorable conditions for development of sprite streamers [*Barrington-Leigh et al.*, 2001] and (2) local enhancements of the lightning field due to atmospheric inhomogeneities result in formation of sprite streamers [e.g., *Zabotin and Wright*, 2001].

[3] On the other hand, telescopic imaging of sprites reveals that filamentary luminous structures with a transverse spatial size on the order of tens to a few hundreds of meters are present in sprites [e.g., *Gerken et al.*, 2000; *Gerken and Inan*, 2002, 2003]. The appearance of fine structure is consistent with the streamer theory of air discharges at sprite altitudes [e.g., *Pasko et al.*, 1998; *Liu and Pasko*, 2004, 2005; *Liu et al.*, 2006]. High-speed video observations and multichannel photometric measurements of sprites indicate that the apparent speed of sprite streamers can reach a substantial fraction of the speed of light [*Stanley et al.*, 1999; *Moudry et al.*, 2002, 2003; *McHarg et al.*, 2002; *Marshall and Inan*, 2005; *Cummer et al.*, 2006; *McHarg et al.*, 2007; *Stenbaek-Nielsen et al.*, 2007]. The observational work reported by *McHarg et al.* [2007] and *Stenbaek-Nielsen et al.* [2007] also demonstrates that sprite streamers accelerate and expand during their propagation, and their emissions are enhanced in the region of streamer heads, which is followed by a dark channel and then a relatively strong emission region in the trailing portion of the streamers which continues for periods longer than expected given the natural lifetime of the emitting state. All the aforementioned features of sprite streamers can be reasonably explained in the framework of streamer discharges at low pressures [e.g., *Liu and Pasko*, 2004, 2005; *Liu et al.*, 2006].

[4] Research work has also been devoted to investigating the spectra of sprites. Four emission band systems of $N_2$ and $N_2^+$ from sprites have been documented so far. They are red emissions of the first positive band system of $N_2$ ($1PN_2$) [e.g., *Mende et al.*, 1995; *Hampton et al.*, 1996], blue emissions of second positive band system of $N_2$ ($2PN_2$) and the first negative band system of $N_2^+$ ($1NN_2^+$) [e.g., *Armstrong et al.*, 1998; *Suszcynsky et al.*, 1998], and far-UV emissions of Lyman-Birge-Hopfield (LBH) band system of $N_2$ [*Mende et al.*, 2006]. The spectroscopic studies of sprites provide insightful information about the air discharges, such as the energetics of the electrons, the electric field driving the optical emissions, and the possible chemical processes occurring in sprites [e.g., *Green et al.*, 1996; *Morrill et al.*, 2002; *Bucsela et al.*, 2003; *Kanmae et al.*, 2007]. The possibility of detecting far-UV emissions of NO-$\gamma$ band system from space is discussed by *Liu and Pasko* [2007] on the basis of sprite streamer modeling. A recent, detailed modeling work on sprite streamer chemistry and photochemistry conducted by *Sentman et al.* [2008] suggests that the sprite spectra may also include long-lived signatures from weak atmospheric emissions OI 557.7 nm and $O_2(b^1\Sigma_g^+ \rightarrow X^3\Sigma_g^-)$, and very weak OH Meinel emissions and $O_2(a^1\Delta_g \rightarrow X^3\Sigma_g^-)$ infrared atmospheric emissions.

[5] The first multiwavelength observations of sprites from space are realized by the Imager of Sprites and Upper

**Table 1.** Summary of Emissions From Sprites

| Emission Band System | Transition | Excitation Threshold (eV) | Cross Section Peak Energy (eV) | Natural Lifetime | Quenching Altitude (km) | Lifetime at 70 km Altitude |
|---|---|---|---|---|---|---|
| $1PN_2$ | $N_2(B^3\Pi_g) \rightarrow N_2(A^3\Sigma_u^+)$ | ~7.35 | 12 | 5.9 $\mu$s | ~53 | 5.4 $\mu$s |
| $2PN_2$ | $N_2(C^3\Pi_u) \rightarrow N_2(B^3\Pi_g)$ | ~11 | 14 | 50 ns | ~30 | 50 ns |
| LBH $N_2$ | $N_2(a^1\Pi_g) \rightarrow N_2(X^1\Sigma_g^+)$ | ~8.55 | 17 | 55 $\mu$s | ~77 | 14 $\mu$s |
| $1NN_2^+$ | $N_2^+(B^2\Sigma_u^+) \rightarrow N_2^+(X^2\Sigma_g^+)$ | ~18.8 | 100 | 71 ns | ~48 | 69 ns |

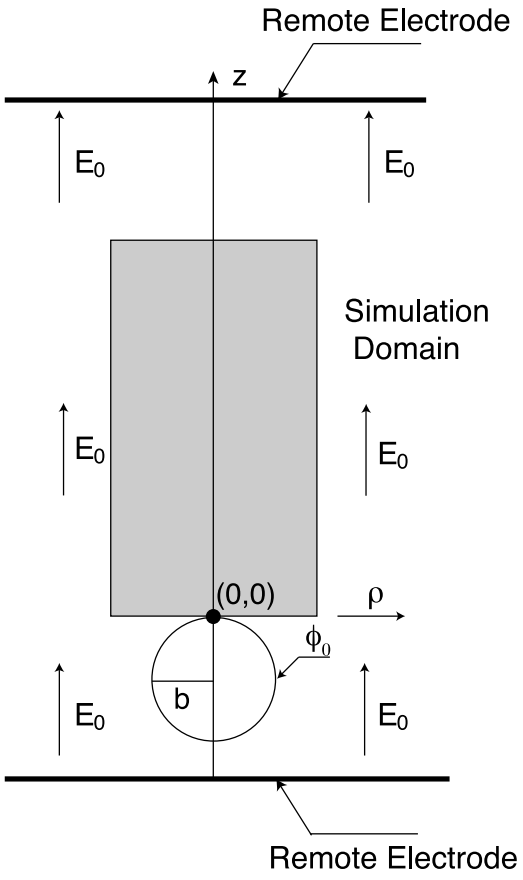


**Figure 2.** The simulation geometry for streamer modeling.

Atmospheric Lightning (ISUAL) scientific payload on the FORMOSAT-2 satellite [*Chern et al.*, 2003; *Mende et al.*, 2005; *Kuo et al.*, 2005; *Mende et al.*, 2006]. The ISUAL payload includes a spectrophotometer with six individual photometer channels covering the spectral range from the far ultraviolet (FUV) to the near infrared. The photometers provide a set of intensity data on emissions from $1PN_2$, $2PN_2$, $N_2$ LBH, and $1NN_2^+$ [*Chern et al.*, 2003; *Mende et al.*, 2005, 2006]. The simultaneous recordings of the emissions from various band systems enable direct comparison between observational data and theoretical sprite models [*Kuo et al.*, 2005; *Liu et al.*, 2006]. The related studies indicate that the tips of streamers are primary emission sources during the early stage of sprites, which is consistent with high-speed video observations [*McHarg et al.*, 2007; *Stenbaek-Nielsen et al.*, 2007], and the strength of the electric field and the mean energy of electrons in the streamer tips are ~3 times of the conventional breakdown field of air and 6.2–9.2 eV, respectively [*Kuo et al.*, 2005; *Liu et al.*, 2006].

[6] The purpose of this paper is to conduct a further comparison of the streamer modeling results with the ISUAL measurements following previous work reported by *Liu et al.* [2006]. We first investigate the intensity ratio between the emissions of $2PN_2$ and $1NN_2^+$ obtained from modeling and observational data. The results indicate that the sprite events considered in the present study were initiated with streamers propagating in electric fields $\sim E_k$. The intensity ratio of $2PN_2$ to $N_2$ LBH is also investigated, and the agreement reached between the modeling results and observational data provides additional information about the poorly known quenching altitude of the upper state $a^1\Pi_g$ of $N_2$ leading to $N_2$ LBH emissions.

## 2. Problem Formulation

### 2.1. Various Emission Band Systems of Sprites

[7] Table 1 summarizes the four emission band systems that have been observed from sprites to date. The lifetimes of the excited states shown in Table 1 include effects of spontaneous transition and quenching [*Pasko et al.*, 1997;

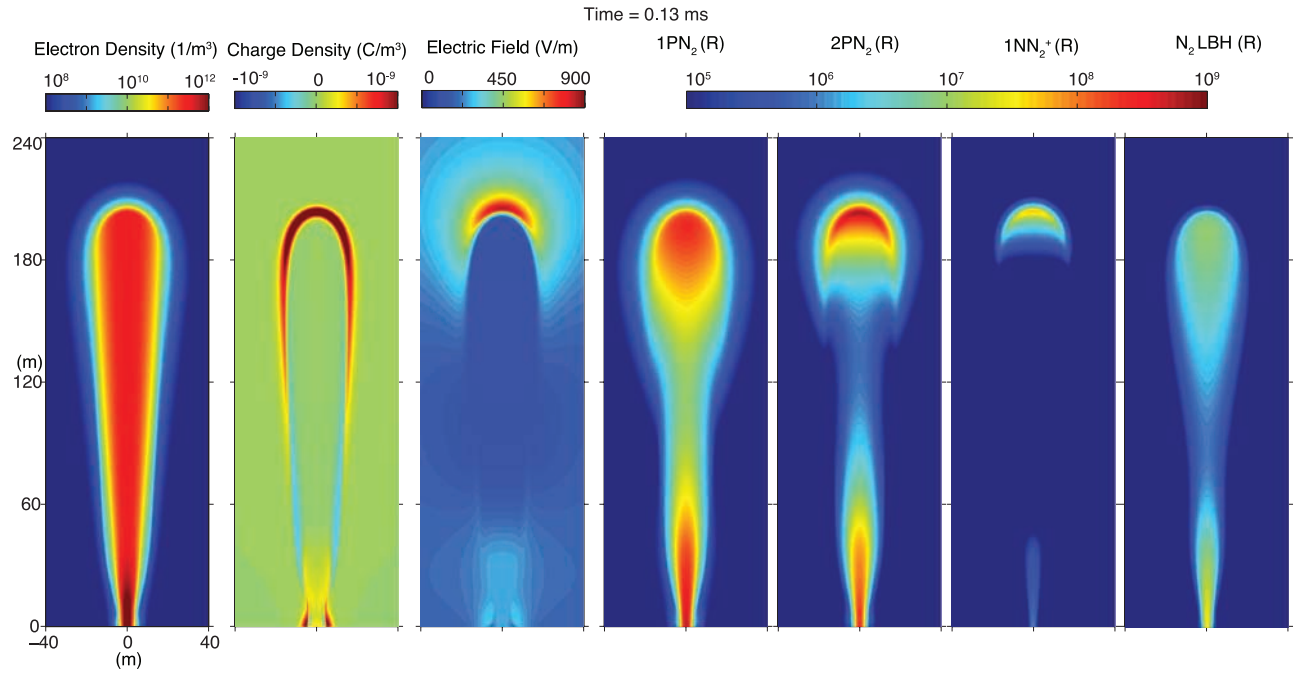


**Figure 3.** A positive streamer propagating in an electric field 30 $N/N_0$ kV/cm at 70 km altitude.

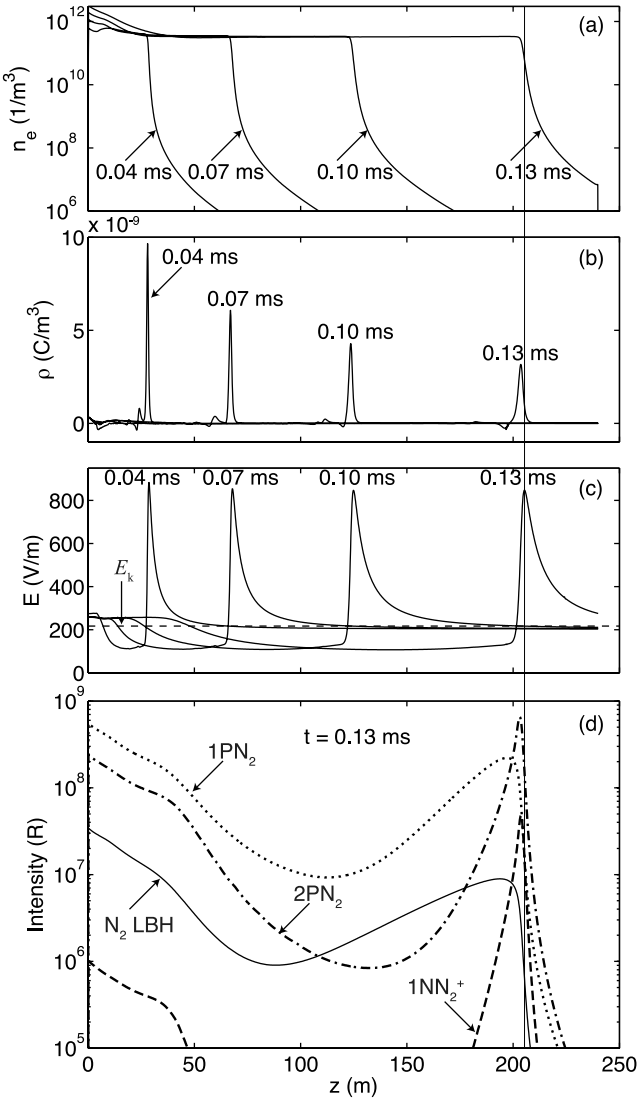


**Figure 4.** The profiles of streamer characteristics along the axis at selected instants of time corresponding to the model streamer shown in Figure 3. (a) The electron density. (b) The electric charge density. (c) The electric field. (d) The intensity of optical emissions (in Rayleighs) at time instant $t = 0.13$ ms. The vertical line represents the location of the peak field.

*Liu and Pasko*, 2004]. The transition and quenching rate coefficients are available from *Vallance-Jones* [1974, p. 119] except those utilized to calculate the lifetime and quenching altitude of $N_2$ ($a^1\Pi_g$) state leading to LBH emissions, a discussion on which is given by *Liu and Pasko* [2005]. A range for the quenching altitude of $N_2$ ($a^1\Pi_g$) state is given as <95 km by *Vallance-Jones* [1974, p. 119] and we obtain a more accurate estimate of this altitude in the present paper.

### 2.2. Temporal Development of Sprites

[8] According to high-speed video observations of sprites [*Stanley et al.*, 1999; *Cummer et al.*, 2006; *McHarg et al.*, 2007; *Stenbaek-Nielsen et al.*, 2007], sprites normally initiate in the altitude range of 75–80 km in a form of downward propagating positive streamers. If there exist upward propagating negative streamers in the observed sprite events, they appear typically 1–2 ms later than the positive streamers and originate from a lower initiation altitude [e.g., *Stenbaek-Nielsen et al.*, 2007]. The comparison study by *Hu et al.* [2007] suggests that the occurrence of bright, short-delayed sprites is well explained by the physical mechanism of sprites proposed by *Pasko et al.* [1997]. This mechanism can be understood by comparing the lightning induced quasi-static electric field at mesospheric/lower ionospheric altitudes with several threshold fields of conventional breakdown theory of air. Solid lines in Figure 1 show the quasi-electrostatic fields produced by lightning discharges with two charge moment changes. The dashed lines show the conventional breakdown threshold field $E_k$ and the minimum fields required for stable propagation of positive ($E_{cr}^+$) and negative ($E_{cr}^-$) streamers. The conventional breakdown threshold field $E_k$ is defined by the equality of the ionization and dissociative attachment coefficients in air [e.g., *Raizer*, 1991, p. 135], which is proportional to the air density. For simplicity, we assume that the similarity law of plasma discharges holds for the fields $E_{cr}^+$ and $E_{cr}^-$, i.e., that the values of $E_{cr}^+$ and $E_{cr}^-$ are proportional to the air density, although experiments on positive streamers indicate that $E_{cr}^+$ may fall off faster with altitude than the decreasing pressure [*Griffiths and Phelps*, 1976]. For the lightning with 1000 C km charge moment change, the lightning field reaches the breakdown threshold field at point A around 75 km altitude, which leads to formation of streamer discharges. Depending on the polarity of CG lightning, either positive or negative streamers are able to propagate downward as long as the local lightning field is greater than the corresponding minimum fields. This implies that positive streamers are able to develop further downward than negative streamers given different polarities but the same strength (in terms of charge moment change) of CG lightning. This argument is supported by fractal modeling results of sprites caused by different polarities of CG lightning [*Pasko et al.*, 2000]. It should be noted that sprites caused by −CG are rarely observed in comparison with those by +CG. Recently, observations of sprite events due to lightning discharges with different polarities but similar strength are reported by *Bailey et al.* [2007], *Thomas et al.* [2008], and *Taylor et al.* [2008]. The authors note that the different termination altitudes of sprites are consistent with the modeling results by *Pasko et al.* [2000]. In the rest of this paper, our discussion focuses on the sprites caused by positive CG (+CG) lightning flashes, which establish an electric field pointing downward above the thunderclouds.

### 2.3. Streamer Model

[9] In this subsection, we give a brief description of the streamer model employed in the present study. The streamer model is axisymmetric. The model equations consist of continuity equations of charged particles and Poisson's equation [*Liu and Pasko*, 2004]. According to Figure 1, the downward propagating sprite streamers develop in an electric field less than $E_k$ except in the region around the initiation point. In order to be able to launch a model streamer and study its characteristics in electric fields less than $E_k$, we utilize the simulation setup shown in Figure 2, which has been used for simulations of streamer discharges at atmospheric pressure [e.g., *Babaeva and Naidis*, 1997]. The applied field $\mathbf{E}_0$ simulates the electric field temporarily established by +CG lightning in the upper atmosphere. This

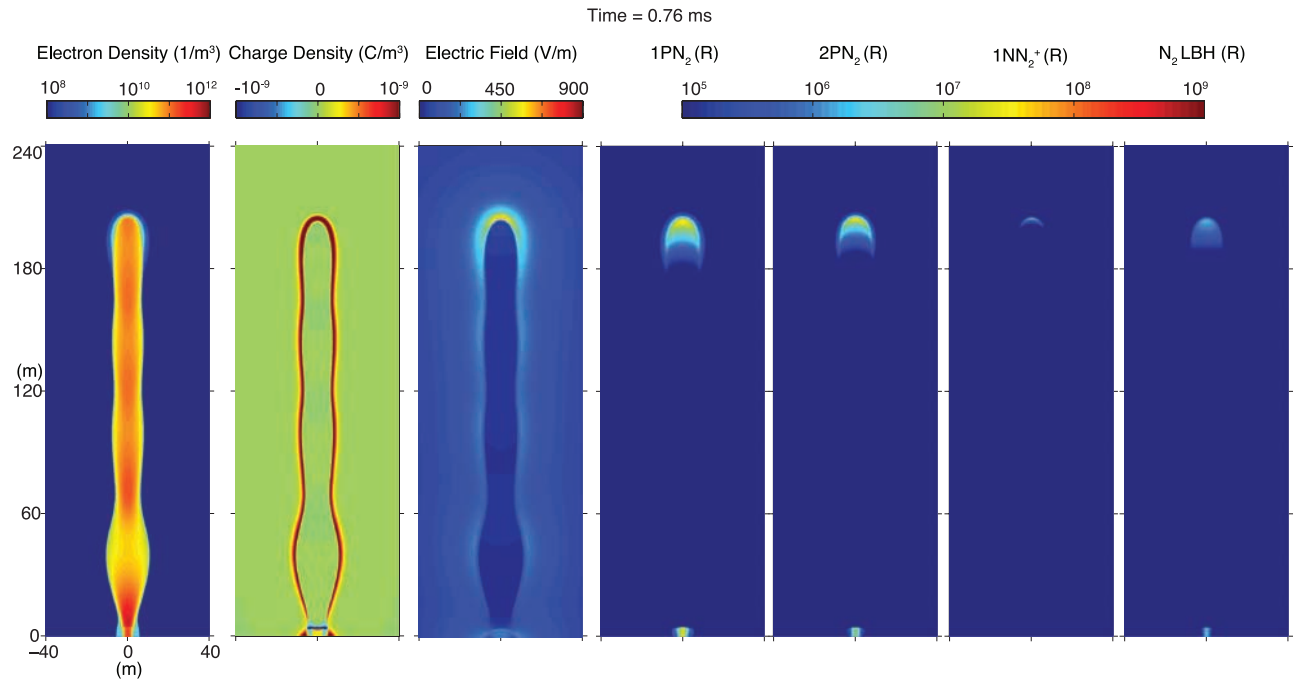


**Figure 5.** A positive streamer propagating in an electric field 5 $N/N_0$ kV/cm at 70 km altitude.

field points in the $z$ direction corresponding to the downward direction in the Earth atmosphere. The small conducting sphere with a radius $b$ and a fixed potential $\phi_0$ strongly enhances the field $\mathbf{E}_0$ in the region near the surface of the sphere. To initiate the streamer, we place a cloud of plasma having spherically symmetric Gaussian spatial distributions with characteristic scale 1.5 m and peak density $5 \times 10^9$ m$^{-3}$ on the axis of symmetry in the vicinity of the sphere. The radius $b$ is 15 m, and the potential $\phi_0$ is determined analytically to obtain the maximum electric field $\sim 3E_k$ at the sphere surface. For a given $E_0$, the maximum field can be calculated as $3E_0 + \phi_0/b$ [*Babaeva and Naidis*, 1997]. The two simulation cases reported in this study are positive streamers developing in $E_0$ = 30 $N/N_0$ kV/cm ($\sim E_k$) and 5 $N/N_0$ kV/cm ($\sim E_{cr}^+$), where $N$ and $N_0$ are neutral densities at the altitude of 70 km and at the ground level, respectively.

### 2.4. Description of the ISUAL Instrument

[10] ISUAL is a scientific payload on the FORMOSAT-2 satellite [*Chern et al.*, 2003; *Mende et al.*, 2005]. The satellite has a Sun-synchronous orbit at an altitude of 891 km and repeatedly passes the same geographic location every solar day. The ISUAL payload is dedicated primarily to observing transient luminous events with a limb-viewing region approximately at midnight local time [*Chern et al.*, 2003; *Mende et al.*, 2005]. The ISUAL payload includes a visible light intensified CCD imager, a bore-sighted six wavelength channel spectrophotometer (SP), and a two channel array photometer (AP). Our present study mainly uses the recordings of the imager and the spectrophotometer, which have a typical time resolution of 30 ms and 0.1 ms, respectively. The six channels of ISUAL spectrophotometer are designed to measure optical emissions in different wavelength ranges. Channels 1, 4 and 6 measure broadband signal within the wavelength range 150–280 nm ($N_2$ LBH), 609–753 nm ($1PN_2$) and 230–410.2 nm (middle UV), respectively. Channels 2, 3 and 5 measure narrowband signal with center wavelength at 337 nm ($2PN_2$), 391.4 nm ($1NN_2^+$) and 777.4 nm (OI), respectively.

## 3. Modeling Results for Positive Streamers at Sprite Altitudes

[11] A straightforward explanation of occurrence of sprites is formation and propagation of streamer discharges when the lightning field reaches the breakdown threshold field of air at mesospheric/lower ionospheric altitudes. We simulate a streamer propagating in a field similar to the breakdown threshold field at a typical sprite altitude 70 km. The corresponding results are presented in Figures 3 and 4. The streamer starts from the lower boundary of the simulation domain and propagates in the direction of the applied field. The magnitude of the applied field $\mathbf{E}_0$ is 30 $N/N_0$ kV/cm and this field points in the $z$ direction shown in Figure 2 (note that this direction coincides with the downward direction in the atmosphere for sprites produced by +CGs). The electron density distribution shows the streamer channel looks like an expanding cone where the electron density is many orders of magnitude larger than the ambient lower ionospheric values ($\sim 10^{-2}$–$10^{-1}$ cm$^{-3}$ [e.g., *Pasko and Stenbaek-Nielsen*, 2002, Figure 4]). During the entire simulation period, there is no clear decay of the electron density in the channel. There exists a shell of charge around the streamer channel and the streamer head. The peak of the charge density decreases with time, but the width of charge density increases with time. In the channel, the charge density is very small and the plasma is in a neutral state. As a result, the electric field is screened out of the channel while a strong enhancement of the field appears in the streamer head. The peak field is slightly greater than $4E_k$. The distributions of different optical emissions are confined to the regions coinciding with the maximum electric field in the streamer head.

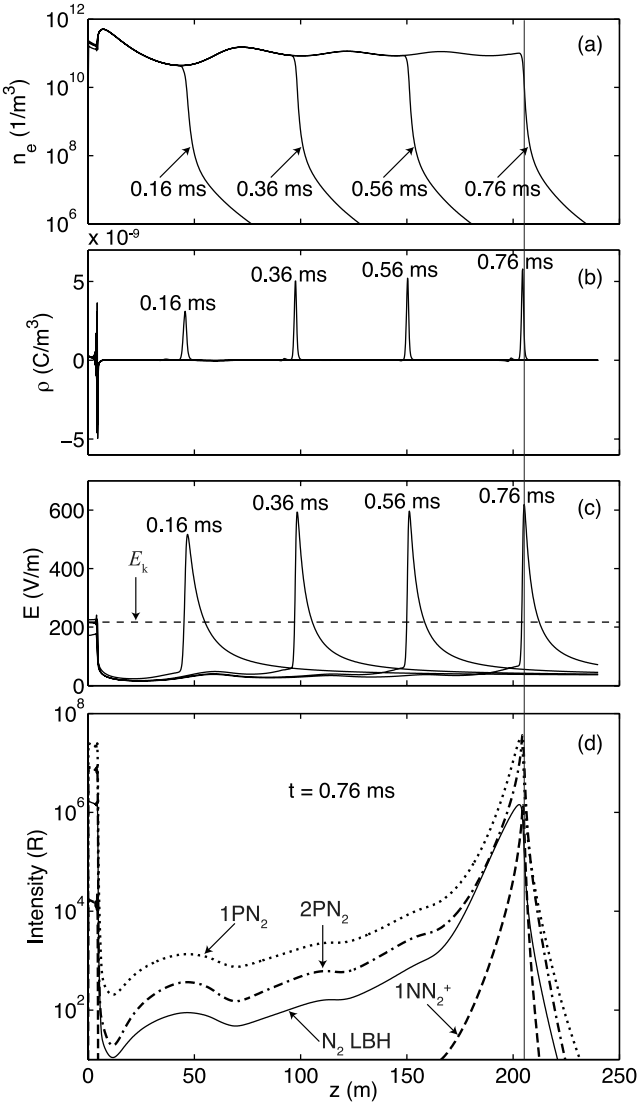


**Figure 6.** The profiles of streamer characteristics along the axis at selected instants of time corresponding to the model streamer shown in Figure 5. (a) The electron density. (b) The electric charge density. (c) The electric field. (d) The intensity of optical emissions (in Rayleighs) at time instant $t = 0.76$ ms. The vertical line represents the location of the peak field.

The variation of the size and sharpness of the enhancement is due to different excitation energy thresholds and lifetimes of the upper states of $N_2$ and $N_2^+$ [e.g., *Liu and Pasko*, 2004, 2005; *Liu et al.*, 2008] (see Table 1).

[12] According to Figure 1, the propagating streamers in electric fields less than the breakdown threshold field are likely to occupy the sprite volume at altitudes below the initiation point. We simulate a positive streamer propagating in an electric field close to the minimum field required for the stable propagation of a positive streamer at 70 km altitude. The corresponding results are presented in Figures 5 and 6. The applied field $\mathbf{E}_0$ has a magnitude 5 $N/N_0$ kV/cm and is directed in the same direction as in the previous modeling case. Similar to the results for the streamer in the strong field, the decay of electron density in the channel is negligible and a positive charge shell surrounds the streamer channel. The electric field and various emissions are highly enhanced in the streamer head. The maximum electric field (about $3E_k$) and emission intensity are much less than those for the strong field case, and the channel field is also much smaller for this case, which results in very different channel profiles for the optical emissions in comparison with the strong field case.

[13] The speeds of the two modeled streamers are compared in Figure 7. High-speed sprite streamers, in the range of $10^6$–$10^7$ m/s, have been observed in several works [*Stanley et al.*, 1999; *Moudry et al.*, 2002, 2003; *McHarg et al.*, 2002; *Marshall and Inan*, 2005; *Cummer et al.*, 2006; *McHarg et al.*, 2007; *Stenbaek-Nielsen et al.*, 2007]. The high-speed sprite video observations reported by *McHarg et al.* [2007] and *Stenbaek-Nielsen et al.* [2007] also show that the acceleration of sprite streamers is as large as $10^{10}$ m/s$^2$ normally occurring during the very early stage of the sprite development. According to Figure 7, the speed of the streamer in the weak applied field varies slightly around $3.0 \times 10^5$ m/s after it is formed, while the streamer for the strong field case accelerates with an increasing acceleration. The streamer speed for the strong field case reaches $3.0 \times 10^6$ m/s at the end of the simulation, and the acceleration is about $2 \times 10^{10}$ m/s$^2$ on average during the entire simulating period agreeing with the observed values by *McHarg et al.* [2007] and *Stenbaek-Nielsen et al.* [2007]. From this comparison, it is clear that the modeling case with an external field of 30 $N/N_0$ kV/cm better explains the observed speed and acceleration than the case with an external field of 5 $N/N_0$ kV/cm.

## 4. ISUAL Data

[14] Our comparison study focuses on three band systems of emissions: $2PN_2$, $1NN_2^+$, and $N_2$ LBH. Each channel of the ISUAL spectrophotometer detects only a fraction of the emissions of the targeted band system. To recover the total emission intensity for individual band systems from the ISUAL measurements, we use the data provided by *Mende et al.* [2005, Table 2] for the intensity fraction of $2PN_2$ and $1NN_2^+$ emissions measured by the channels 2 and 3 of the ISUAL spectrophotometer. We ignore the contribution from $1NN_2^+$ emission band system to the channel 2, because its intensity is much weaker than that of $2PN_2$. As a result, channel 2 records 27.8% of the total emission intensity of $2PN_2$ and channel 3 records 66% of $1NN_2^+$. For channel 1, we combine the channel filter responsivity profile with the atmosphere transmittance for an observation geometry assuming 70 km source altitude and a mean distance about 2500 km from the source to the satellite to obtain 11% of the total LBH emission intensity measured by this channel [*Liu et al.*, 2006].

[15] The first sprite event was observed on 18 July 2004. The same event has been analyzed in several previous studies [e.g., *Mende et al.*, 2005; *Kuo et al.*, 2005]. The event was triggered at 2130:15.316 UT following the causative lightning occurring at 2130:15.310 UT. Figure 8 shows the image of the sprite event and the recordings of the first three spectrophotometric channels after removing the background noise, which is approximated by an average value of each channel in a 5 ms time interval about 10 ms before the lightning. For the 391.4 nm channel, the sprite signal is

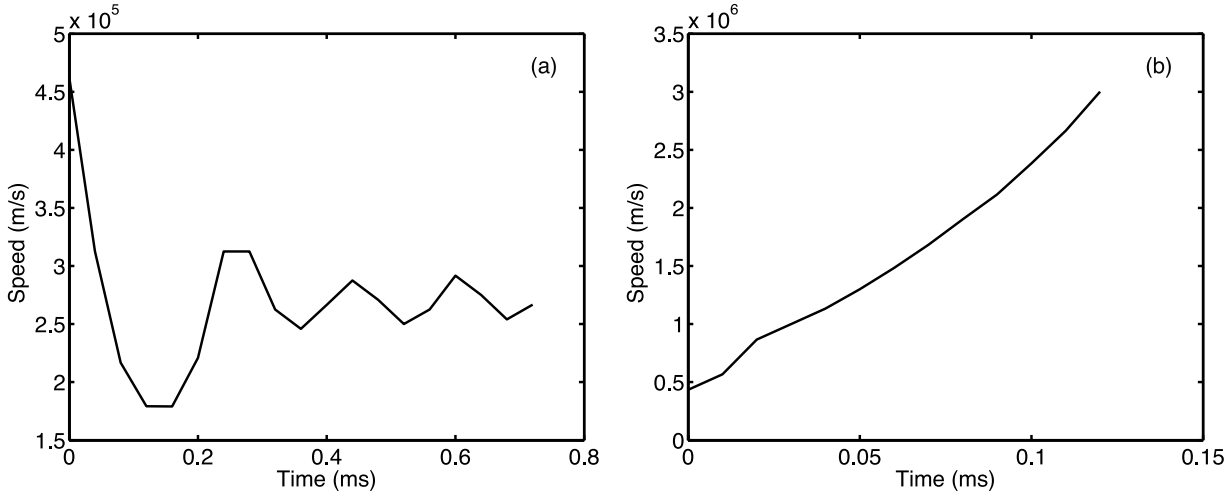


**Figure 7.** The speed of the model sprite streamer at 70 km altitude as a function of time: (a) the case for an applied field 5 $N/N_0$ kV/cm and (b) the case for an applied field 30 $N/N_0$ kV/cm.

largely contaminated by the lightning. The contribution of the lightning to the signal is estimated by the solid line shown in Figure 9a, and Figure 9b shows the result after subtracting the lightning contribution from the data for the 391.4 nm channel. The solid line represents an exponentially decaying function with a second-order polynomial of time as its exponent: $I = \exp(a_1 t^2 + a_2 t + a_3)$. To obtain the three $a_j$ coefficients, a decay interval of lightning emissions is first identified by setting the start and end moments of time. The coefficients are obtained by fitting a natural logarithm of the ISUAL data in this interval using an MATLAB function polyfit. Because of the variability of the time lag between lightning and sprites, the best fit of the data points is found by trial and error with different lightning decay intervals. For the event shown by Figure 8, the start and end of the lightning decay interval are −4.0 and −0.3 ms, respectively.

[16] As another example, a second sprite event was recorded following the same trigger for the event shown in Figure 8. The image and spectrophotometric signatures are shown in Figure 10. The start and end of the lightning decay are set at −2.0 and −0.3 ms, respectively. Figure 11 shows that the employed fitting procedure gives a reasonable estimate to the lightning decay signal. However, we have noted that the fitting procedure may result in inaccurate estimates of the lightning contribution to the overall signal at the later moments of time during sprite events.

[17] Besides the two sprite events following the trigger at 2130:15.316 UT on 18 July 2004, we use the ISUAL data for one additional sprite event for our comparison study. This event was detected at 2322:30.623 UT on 6 March 2005. The spectrophotometric data for this event show no lightning signatures. Therefore for this event we remove

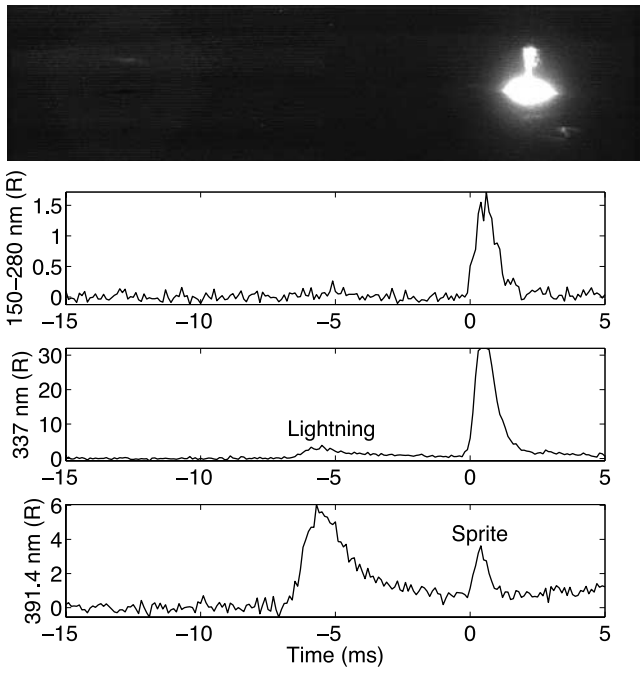


**Figure 8.** A sprite event detected by ISUAL at 2130:15.316 UT on 18 July 2004.

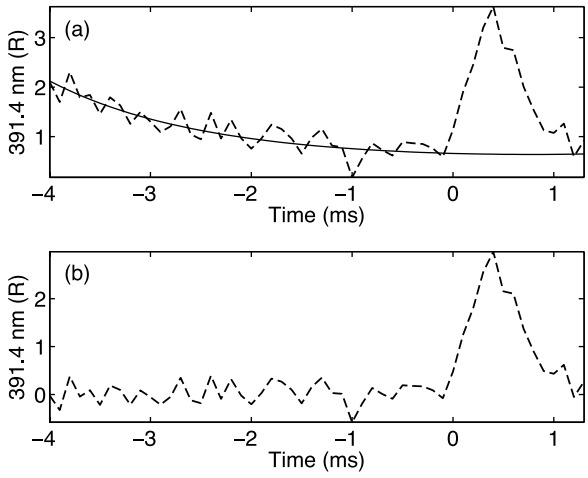


**Figure 9.** Comparison of the signal of the 391.4 nm channel (a) before and (b) after removing the lightning contamination.

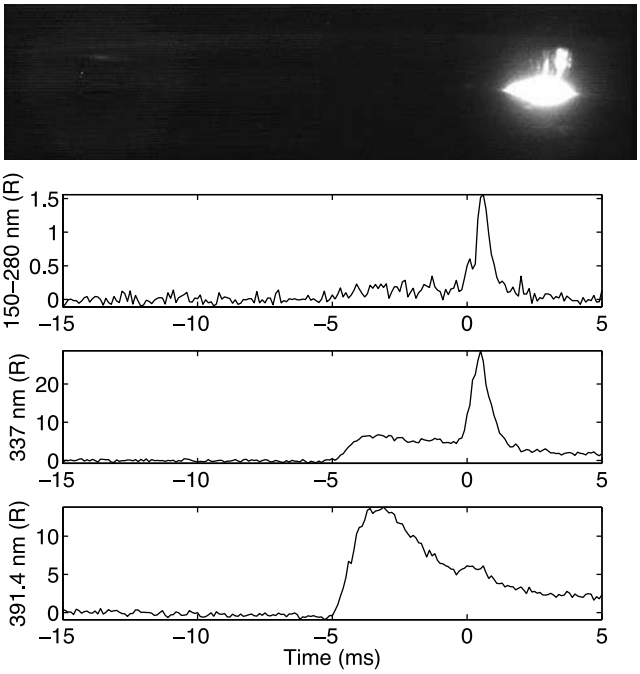


**Figure 10.** A second sprite event detected by ISUAL following the trigger at 2130:15.316 UT on 18 July 2004.

only the background noise from the spectrophotometric data.

## 5. Results

### 5.1. Intensity Ratio of $2PN_2$ to $1NN_2^+$

[18] The excitation frequencies of the upper states of $N_2(B^3\Pi_g)$, $N_2(C^3\Pi_u)$, $N_2(a^1\Pi_g)$ and $N_2^+(B^2\Sigma_u^+)$ are very sensitive to the magnitude of the driving electric field [*Liu and Pasko*, 2005, Figure 1a]. As demonstrated previously with relationship to laboratory as well as sprite discharges, it is possible to utilize the intensity ratio between two emission band systems to derive the information on the electric field driving the emission source [e.g., *Gallimberti et al.*, 1974; *Teich*, 1993; *Green et al.*, 1996; *Morrill et al.*, 1998; *Armstrong et al.*, 1998; *Morrill et al.*, 2002; *Simek*, 2002; *Pasko*, 2007, and references therein]. We investigate the intensity ratio of $2PN_2$ to $1NN_2^+$ obtained from modeling and ISUAL observations to extract the information about the lightning field driving sprite phenomenon at 70 km altitude.

[19] Choosing the intensity ratio of $2PN_2$ to $1NN_2^+$ as our comparison quantity has several advantages:

[20] 1. The intensity ratio obtained for a single streamer reasonably represents the same quantity for the entire sprite event [*Liu et al.*, 2006].

[21] 2. The quenching altitudes of $N_2(C^3\Pi_u)$ to $N_2^+(B^2\Sigma_u^+)$ are 30 and 48 km, respectively. For sprites with high termination altitude (>48 km) or sprites at the early stage of development, the quenching effects on this ratio are minimal.

[22] 3. The two ISUAL spectrophotometric channels devoted to measuring $2PN_2$ to $1NN_2^+$ centered at the wavelengths 337 and 391.4 nm, respectively. At these wavelengths, the atmospheric effects (i.e., attenuation) can be ignored [e.g., *Mende et al.*, 2005; *Kuo et al.*, 2005; *Liu and Pasko*, 2005]. According to the modeling work by *Liu and Pasko* [2004], streamers at pressures lower than several Torr (i.e., above 40 km altitude) satisfy similarity laws. Following the arguments presented by *Liu et al.* [2006], the relative strength of emissions of $2PN_2$ and $1NN_2^+$ is the same for the sprite streamers in the region >48 km if the ambient reduced electric field is the same. In other words, if we obtain the intensity ratio of $2PN_2$ to $1NN_2^+$ for a streamer in the reduced field 30 $N/N_0$ kV/cm at 70 km altitude, the same ratio is applicable for a sprite streamer in the same reduced field at any altitude >48 km.

[23] However, the intensity ratios corresponding to the streamer head and the streamer channel are different [*Liu and Pasko*, 2005]. We therefore consider the ratios between the total (i.e., integrated over entire streamer body) emission intensities. The calculated total emission intensities represent total number of photons emitted per second, and related ratios can be directly compared to similar ratios derived from ISUAL spectrophotometric data.

[24] Figure 12 shows the intensity ratio of $2PN_2$ to $1NN_2^+$ obtained using streamer modeling results and ISUAL spectrophotometric data. The streamer developing in the strong field propagates very fast, and it takes about 0.15 ms for the streamer to move through the entire simulation domain. In contrast, the time required for the streamer in the weak electric field to transverse the simulation domain is about 1 ms. Therefore, the ratio from the modeling results shown in Figure 12 is available up to about 0.15 ms for the strong field case and for a longer time interval for the weak field case. After the initial formation of the streamer in the high field region around the conducting sphere, the ratios from modeling results show only small variation over time. Within ~0.2 ms of the initial stage of the three sprite events, the intensity ratios from ISUAL spectrophotometric data agree better with the modeling results for the strong field case than for the weak field case. An important conclusion which arises from this result is that the sprites under study are initiated by streamers developing in electric fields $\sim E_k$,

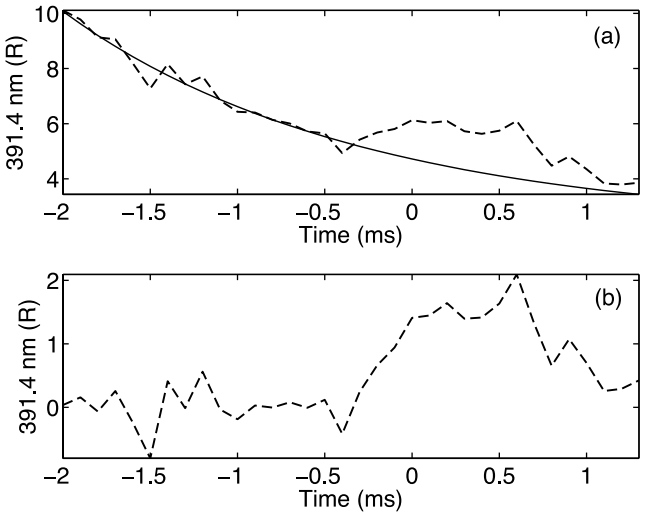


**Figure 11.** Comparison of the signal of the 391.4 nm channel (a) before and (b) after removing the lightning contamination for the sprite event shown in Figure 10.

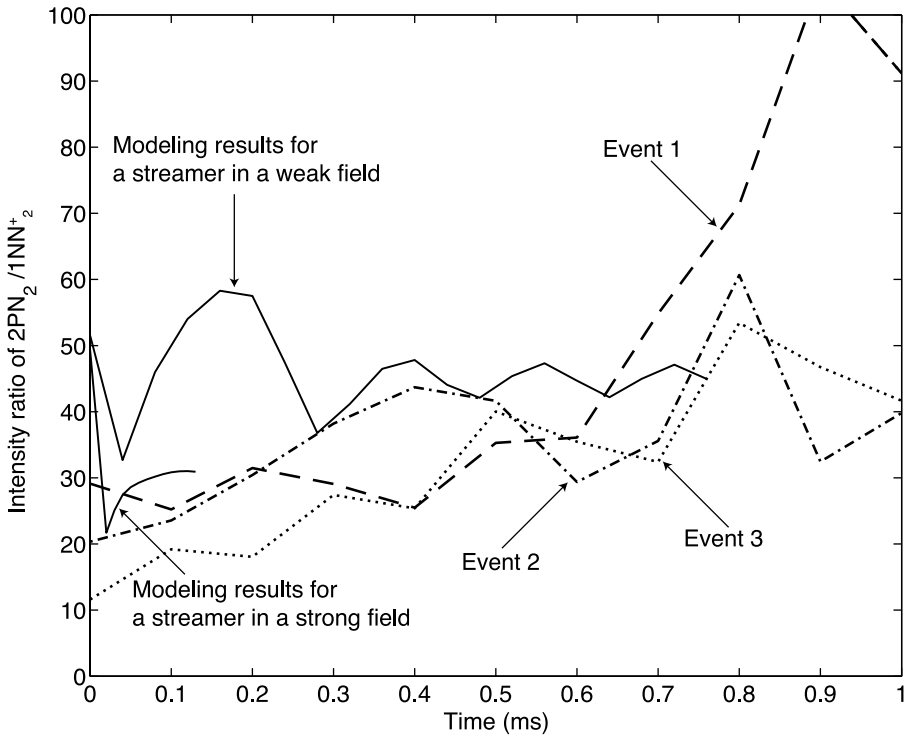


**Figure 12.** Intensity ratio $2PN_2/1NN_2^+$ as a function of time computed using streamer modeling results and ISUAL spectrophotometric measurements. The streamers in strong and weak fields correspond to those presented in Figures 3 and 5, respectively. Events 1 and 2 correspond to Figures 8 and 10, respectively. Event 3 is a sprite event triggered at 2322:30.623 UT on 6 March 2005.

or the sprite events are initiated when the lightning electric field reaches $E_k$. This result is consistent with the physical mechanism of sprites advanced by *Pasko et al.* [1997] and the comparison study conducted recently by *Hu et al.* [2007] between modeling results of lightning fields obtained using measured current moments and sprite video observations.

### 5.2. Intensity Ratio of $2PN_2$ to $N_2$ LBH

[25] As discussed by *Liu and Pasko* [2005], the present knowledge on quenching rates of the upper state $a^1\Pi_g$ leading to $N_2$ LBH emissions is very limited. The following analysis provides a verification for the result that the quenching altitude of $N_2(a^1\Pi_g)$ state is ~77 km [*Liu and Pasko*, 2005]. We make two assumptions: (1) The initiation altitude of sprites is 75–80 km and (2) about 11% of the total LBH emissions is measured by channel 1 of the ISUAL spectrophotometer.

[26] Figure 13 shows the intensity ratios of $2PN_2$ to $N_2$ LBH obtained using streamer modeling results and ISUAL spectrophotometric data. The solid line corresponds to the positive streamer developing in a strong field (Figure 3) at 70 km altitude. According to the discussion in section 5.1, within the initial 0.2 ms of sprite development, emissions from streamers propagating in strong fields are representative of the emissions from the entire sprite. The intensity ratio of $2PN_2$ to $1NN_2^+$ is independent of altitude, so that we can directly compare the modeling results for a positive streamer at 70 km altitude to measured emissions coming from altitude at which sprite was initiated during the initial 0.2 ms of the sprite event. To compare the intensity ratios of $2PN_2$ to $N_2$ LBH, we must take into account the quenching effects, because the initiation altitude of sprites is different from the altitude at which the streamer is modeled. If we consider that the sprite event is initiated with streamer development at an altitude of 77 km (the initiation altitude range is 75–80 km), the intensity ratio is decreased approximately by a factor of $e$, because the intensity of $N_2$ LBH emissions increases by the same factor. The result of applying this modification is shown by the blue solid line in Figure 13. The blue line is near the lower bottom of the ratios obtained from ISUAL measurements.

[27] The second assumption made for this analysis is related to observation geometry: the sprite altitude is 70 km and the distance between the satellite and the sprite is 2500 km [*Liu and Pasko*, 2005, Figure 3]. The percentage of the total intensity of LBH emissions measured by channel 1 varies with different observation geometries. If the sprite altitude is higher than 70 km or the distance between the sprite and the satellite is shorter than 2500 km, the measured fraction of LBH emissions increases slightly; otherwise, the fraction decreases. If we consider a source at 77 km altitude viewed at two extreme locations of the field of view of the spectrophotometer: at the near edge, 2370 km away, and at the limb, 3370 km away [*Kuo et al.*, 2007], the fraction of the total LBH emissions from the source detected by channel 1 varies from 0.8 to 1.2 shifting the ISUAL ratios in Figure 13 either up or down by about 20%.

[28] Additionally, we assumed that the $N_2$ $a^1\Pi_g$ state is produced by electron impact excitation only and ignored the radiative and collisional cascading between $N_2$ singlet states $a^1\Pi_g$, $a'^1\Sigma_u^-$ and $w^1\Delta_u$. The two singlets $a'^1\Sigma_u^-$ and $w^1\Delta_u$

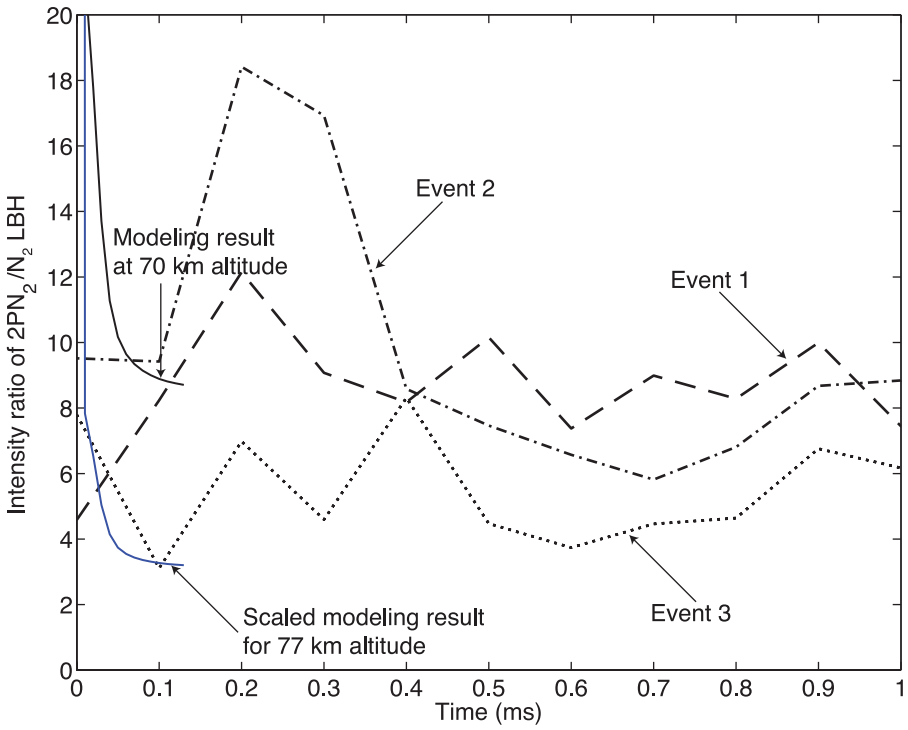


**Figure 13.** Intensity ratio $2PN_2/N_2$ LBH as a function of time computed using streamer modeling results and ISUAL spectrophotometric measurements. The black solid line corresponds to the streamer at 70 km altitude in a strong electric field presented in Figure 3, and the blue solid line shows the intensity ratio obtained by scaling the modeling results to 77 km altitude taking into account the quenching effects. Events 1 and 2 correspond to Figures 8 and 10, respectively. Event 3 is a sprite event triggered at 2322:30.623 UT on 6 March 2005. Because of the variability in viewing geometries, the ISUAL ratios could shift up or down by about 20%.

have a much longer natural lifetimes than $a^1\Pi_g$ and their quenching rates by atmospheric species $N_2$, $O_2$, and O are either on the same order or less than those of $a^1\Pi_g$ state [*Eastes*, 2000]. According to modeling studies on UV emissions of dayglow and aurora [*Eastes and Dentamaro*, 1996; *Eastes*, 2000], the total emission from the $N_2$ LBH band system increases if the radiative and collisional energy transfer between those three singlet states is taken into account. The factor of the increase depends on altitude because the relative direct excitation of the three singlets in dayglow and aurora varies with altitude, and it reaches a maximum 1.67 at altitudes >200 km and drops to about 1.1 at an altitude of 100 km [*Eastes*, 2000, Figure 4]. Given that electron impact cross section for excitation of $N_2$ $a^1\Pi_g$ state is generally larger than the sum of the cross sections of the other two singlet states (see the cross sections compiled by A. V. Phelps, http://jilawww.colorado.edu/~avp/collision_data), the number 1.67 also represents the maximum possible enhancement factor of the total $N_2$ LBH emissions at sprite altitudes due to the radiative and collisional energy transfer between those three singlet states.

[29] It follows from the above discussion that the coupling of $N_2$ singlet states and the variability in viewing conditions would change the results shown by Figure 13, but not significantly. Ideally, the modeling results should be located in the middle of the range bounded by the ISUAL ratios in Figure 13, which can be realized by increasing the quenching altitude of $N_2$ $a^1\Pi_g$ state by about 7 km, i.e., reducing the total emissions of $N_2$ LBH by a factor of $e$. On the other hand, as positive streamers propagate downward after initiation, the source altitude is decreasing. Given the observed speed of streamers (on the order of $10^7$ m/s in initial stage of sprites), they can move 7 km within several milliseconds, which suggests that the ISUAL measurements should be well bounded by the modeling results at 70 km and 77 km altitudes, as shown by Figure 13. We therefore conclude that 77 km is a good estimate for the quenching altitude of the $N_2$ $a^1\Pi_g$ state, and that given factors discussed above the quenching altitude could in principle be several kilometers higher than 77 km.

## 6. Summary and Conclusions

[30] The modeling results for positive streamers propagating in two different fields: 30 $N/N_0$ and 5 $N/N_0$ kV/cm indicate that although the streamers are able to continue developing in these two fields, the characteristics of the streamers, for example the relative strength of different emission band systems and the speeds of the streamers, are different. We compare the intensity ratio of $2PN_2$ to $1NN_2$ obtained from sprite streamer modeling with the same ratio derived from ISUAL spectrophotometric data. The comparison shows that the ratio obtained for the streamer developing in the field 30 $N/N_0$ ($\sim E_k$) agrees better with the ISUAL measurements at the very early stage of the sprite development than for the streamer in the field 5 $N/N_0$

($\sim E_{cr}^{+}$). This finding implies that the sprite events analyzed in our study are very likely initiated with streamers propagating in strong electric fields such as $E_k$; that is, the quasi-static electric field produced by the lightning in the upper atmosphere reaches the local conventional breakdown threshold field. Our results support the sprite theory advanced by *Pasko et al.* [1997] that sprites are caused by conventional breakdown of air when the lightning field in the upper atmosphere exceeds the local breakdown threshold field, which has also been supported by a recent study comparing modeled lightning fields obtained using measured current moments of causative lightning discharges and video observations of sprites [*Hu et al.*, 2007].

[31] Knowing that emissions from sprites at the stage of their initial development are well explained by the radiation coming from streamers in strong fields, we compare the intensity ratio of $2PN_2$ to $N_2$ LBH obtained from the model streamer in the strong field with the ISUAL data for the same sprite events. The intensity ratio of $2PN_2$ to $N_2$ LBH depends on the altitude of the emission source because of quenching effects. The scaled ratio from the model streamer at 70 km to a typical 77 km initiation altitude of sprites reasonably agrees with the ISUAL data. Our results support the fact that the quenching altitude of $N_2$ ($a^1\Pi_g$) is about 77 km as suggested by *Liu and Pasko* [2005].

[32] **Acknowledgments.** This research was supported by the Physics and Space Sciences Department of Florida Institute of Technology and by NSF grants ATM 0725360 and ATM 0734083 to Penn State University.

[33] Wolfgang Baumjohann thanks Jeff Morrill and Davis Sentman for their assistance in evaluating this paper.

## References

Armstrong, R. A., J. A. Shorter, M. J. Taylor, D. M. Suszcynsky, W. A. Lyons, and L. S. Jeong (1998), Photometric measurements in the SPRITES' 95 and 96 campaigns of nitrogen second positive (399.8 nm) and first negative (427.8 nm) emission, *J. Atmos. Sol. Terr. Phys.*, *60*, 787–799.

Babaeva, N. Y., and G. V. Naidis (1997), Dynamics of positive and negative streamers in air in weak uniform electric fields, *IEEE Trans. Plasma Sci.*, *25*, 375–379.

Bailey, M. A., M. J. Taylor, P. D. Pautet, S. A. Cummer, N. Jaugey, J. N. Thomas, and R. H. Holzworth (2007), Sprite halos and associated lightning characteristics over South America, *Eos Trans. AGU*, *88*(52), Fall Meet. Suppl., Abstract AE23A-0896.

Barrington-Leigh, C. P., U. S. Inan, and M. Stanley (2001), Identification of sprites and elves with intensified video and broadband array photometry, *J. Geophys. Res.*, *106*(A2), 1741–1750, doi:10.1029/2000JA000073.

Boccippio, D. J., E. R. Williams, S. J. Heckman, W. A. Lyons, I. T. Baker, and R. Boldi (1995), Sprites, ELF transients, and positive ground strokes, *Science*, *269*, 1088–1091.

Bucsela, E., J. Morrill, M. Heavner, C. Siefring, S. Berg, D. Hampton, D. Moudry, E. Wescott, and D. Sentman (2003), $N_2(B^3\Pi_g)$ and $N_2^+(A^2\Pi_u)$ vibrational distributions observed in sprites, *J. Atmos. Sol. Terr. Phys.*, *65*, 583–590.

Chern, J. L., R. R. Hsu, H. T. Su, S. B. Mende, H. Fukunishi, Y. Takahashi, and L. C. Lee (2003), Global survey of upper atmospheric transient luminous events on the ROCSAT-2 satellite, *J. Atmos. Sol. Terr. Phys.*, *65*, 647–659, doi:10.1016/S1364-6826(02)00317-6.

Cummer, S. A., N. C. Jaugey, J. B. Li, W. A. Lyons, T. E. Nelson, and E. A. Gerken (2006), Submillisecond imaging of sprite development and structure, *Geophys. Res. Lett.*, *33*, L04104, doi:10.1029/2005GL024969.

Eastes, R. W. (2000), Modeling the $N_2$ Lyman-Birge-Hopfield bands in the dayglow: Including radiative and collisional cascading between the singlet states, *J. Geophys. Res.*, *105*(A8), 18,557–18,573, doi:10.1029/1999JA00378.

Eastes, R. W., and A. V. Dentamaro (1996), Collision-induced transitions between the $a^1\Pi_g$, $a'^1\sum_u^-$, and $w^1\Delta_u$ states of $N_2$: Can they affect auroral $N_2$ Lyman-Birge-Hopfield band emissions?, *J. Geophys. Res.*, *101*, 26,931–26,940, doi:10.1029/96JA01636.

Gallimberti, I., J. K. Hepworth, and R. C. Klewe (1974), Spectroscopic investigation of impulse corona discharges, *J. Phys. D Appl. Phys.*, *7*, 880–899.

Gerken, E. A., and U. S. Inan (2002), A survey of streamer and diffuse glow dynamics observed in sprites using telescopic imagery, *J. Geophys. Res.*, *107*(A11), 1344, doi:10.1029/2002JA009248.

Gerken, E. A., and U. S. Inan (2003), Observations of decameter-scale morphologies in sprites, *J. Atmos. Sol. Terr. Phys.*, *65*, 567–572, doi:10.1016/S1364-6826(02)00333-4.

Gerken, E. A., U. S. Inan, and C. P. Barrington-Leigh (2000), Telescopic imaging of sprites, *Geophys. Res. Lett.*, *27*, 2637–2640.

Green, B. D., M. E. Fraser, W. T. Rawlins, L. Jeong, W. A. M. Blumberg, S. B. Mende, G. R. Swenson, D. L. Hampton, E. M. Wescott, and D. D. Sentman (1996), Molecular excitation in sprites, *Geophys. Res. Lett.*, *23*, 2161–2164.

Griffiths, R. F., and C. T. Phelps (1976), The effects of air pressure and water vapor content on the propagation of positive corona streamers, and their implications to lightning initiation, *Q. J. R. Meteorol. Soc.*, *102*, 419–426.

Hampton, D. L., M. J. Heavner, E. M. Wescott, and D. D. Sentman (1996), Optical spectral characteristics of sprites, *Geophys. Res. Lett.*, *23*, 89–93.

Hu, W. Y., S. A. Cummer, and W. A. Lyons (2007), Testing sprite initiation theory using lightning measurements and modeled electromagnetic fields, *J. Geophys. Res.*, *112*, D13115, doi:10.1029/2006JD007939.

Kanmae, T., H. C. Stenbaek-Nielsen, and M. G. McHarg (2007), Altitude resolved sprite spectra with 3 ms temporal resolution, *Geophys. Res. Lett.*, *34*, L07810, doi:10.1029/2006GL028608.

Kuo, C. L., R. R. Hsu, H. T. Su, A. B. Chen, L. C. Lee, S. B. Mende, H. U. Frey, H. Fukunishi, and Y. Takahashi (2005), Electric fields and electron energies inferred from the ISUAL recorded sprites, *Geophys. Res. Lett.*, *32*, L19103, doi:10.1029/2005GL023389.

Kuo, C. L., et al. (2007), Modeling elves observed by FORMOSAT-2 satellite, *J. Geophys. Res.*, *112*, A11312, doi:10.1029/2007JA012407.

Liu, N. Y., and V. P. Pasko (2004), Effects of photoionization on propagation and branching of positive and negative streamers in sprites, *J. Geophys. Res.*, *109*, A04301, doi:10.1029/2003JA010064.

Liu, N. Y., and V. P. Pasko (2005), Molecular nitrogen LBH band system far-UV emissions of sprite streamers, *Geophys. Res. Lett.*, *32*, L05104, doi:10.1029/2004GL022001.

Liu, N. Y., and V. P. Pasko (2007), Modeling studies of NO-$\gamma$ emissions of sprites, *Geophys. Res. Lett.*, *34*, L16103, doi:10.1029/2007GL030352.

Liu, N. Y., et al. (2006), Comparison of results from sprite streamer modeling with spectrophotometric measurements by ISUAL instrument on FORMOSAT-2 satellite, *Geophys. Res. Lett.*, *33*, L01101, doi:10.1029/2005GL024243.

Liu, N. Y., S. Célestin, A. Bourdon, V. P. Pasko, P. Ségur, and E. Marode (2008), Photoionization and optical emission effects of positive streamers in air at ground pressure, *IEEE Trans. Plasma Sci.*, *36*(4), 942–943.

Marshall, R. A., and U. S. Inan (2005), High-speed telescopic imaging of sprites, *Geophys. Res. Lett.*, *32*, L05804, doi:10.1029/2004GL021988.

McHarg, M. G., R. K. Haaland, D. R. Moudry, and H. C. Stenbaek-Nielsen (2002), Altitude-time development of sprites, *J. Geophys. Res.*, *107*(A11), 1364, doi:10.1029/2001JA000283.

McHarg, M. G., H. C. Stenbaek-Nielsen, and T. Kammae (2007), Streamer development in sprites, *Geophys. Res. Lett.*, *34*, L06804, doi:10.1029/2006GL027854.

Mende, S. B., R. L. Rairden, G. R. Swenson, and W. A. Lyons (1995), Sprite spectra: $N_2$ 1 PG band identification, *Geophys. Res. Lett.*, *22*, 2633–2637.

Mende, S. B., H. U. Frey, R. R. Hsu, H. T. Su, A. B. Chen, L. C. Lee, D. D. Sentman, Y. Takahashi, and H. Fukunishi (2005), D region ionization by lightning-induced EMP, *J. Geophys. Res.*, *110*, A11312, doi:10.1029/2005JA011064.

Mende, S. B., et al. (2006), Spacecraft based studies of transient luminous events, in *Sprites, Elves and Intense Lightning Discharges*, edited by M. Füllekrug, E. A. Mareev, and M. J. Rycroft, *NATO Sci. Ser., Ser. II*, *225*, 123–149.

Morrill, J. S., E. J. Bucsela, V. P. Pasko, S. L. Berg, W. M. Benesch, E. M. Wescott, and M. J. Heavner (1998), Time resolved $N_2$ triplet state vibrational populations and emissions associated with red sprites, *J. Atmos. Sol. Terr. Phys.*, *60*, 811–829.

Morrill, J., et al. (2002), Electron energy and electric field estimates in sprites derived from ionized and neutral $N_2$ emissions, *Geophys. Res. Lett.*, *29*(10), 1462, doi:10.1029/2001GL014018.

Moudry, D. R., H. C. Stenbaek-Nielsen, D. D. Sentman, and E. M. Wescott (2002), Velocities of sprite tendrils, *Geophys. Res. Lett.*, *29*(20), 1992, doi:10.1029/2002GL015682.

Moudry, D. R., H. C. Stenbaek-Nielsen, D. D. Sentman, and E. M. Wescott (2003), Imaging of elves, halos and sprite initiation at 1 ms time resolution,

*J. Atmos. Sol. Terr. Phys.*, *65*, 509–518, doi:10.1016/S1364-6826(02)00323-1.

Pasko, V. P. (2007), Red sprite discharges in the atmosphere at high altitude: The molecular physics and the similarity with laboratory discharges, *Plasma Sources Sci. Technol.*, *16*, S13–S29, doi:10.1088/0963-0252/16/1/S02.

Pasko, V. P., and H. C. Stenbaek-Nielsen (2002), Diffuse and streamer regions of sprites, *Geophys. Res. Lett.*, *29*(10), 1440, doi:10.1029/2001GL014241.

Pasko, V. P., U. S. Inan, T. F. Bell, and Y. N. Taranenko (1997), Sprites produced by quasi-electrostatic heating and ionization in the lower ionosphere, *J. Geophys. Res.*, *102*(A3), 4529–4561, doi:10.1029/96JA03528.

Pasko, V. P., U. S. Inan, and T. F. Bell (1998), Spatial structure of sprites, *Geophys. Res. Lett.*, *25*, 2123–2126.

Pasko, V. P., U. S. Inan, and T. F. Bell (2000), Fractal structure of sprites, *Geophys. Res. Lett.*, *27*(4), 497–500, doi:10.1029/1999GL010749.

Raizer, Y. P. (1991), *Gas Discharge Physics*, Springer, New York.

Sentman, D. D., E. M. Wescott, D. L. Osborne, D. L. Hampton, and M. J. Heavner (1995), Preliminary results from the Sprites94 campaign: Red sprites, *Geophys. Res. Lett.*, *22*, 1205–1208.

Sentman, D. D., H. C. Stenbaek-Nielsen, M. G. McHarg, and J. S. Morrill (2008), Plasma chemistry of sprite streamers, *J. Geophys. Res.*, *113*, D11112, doi:10.1029/2007JD008941.

Simek, M. (2002), The modelling of streamer-induced emission in atmospheric pressure, pulsed positive corona discharge: $N_2$ second positive and NO-$\gamma$ systems, *J. Phys. D Appl. Phys.*, *35*, 1967–1980.

Stanley, M., P. Krehbiel, M. Brook, C. Moore, W. Rison, and B. Abrahams (1999), High speed video of initial sprite development, *Geophys. Res. Lett.*, *26*, 3201–3204.

Stenbaek-Nielsen, H. C., M. G. McHarg, T. Kammae, and D. D. Sentman (2007), Observed emission rates in sprite streamer heads, *Geophys. Res. Lett.*, *34*, L11105, doi:10.1029/2007GL029881.

Suszcynsky, D. M., R. Roussel-Dupre, W. A. Lyons, and R. A. Armstrong (1998), Blue-light imagery and photometry of sprites, *J. Atmos. Sol. Terr. Phys.*, *60*, 801–809.

Taylor, M. J., et al. (2008), Rare measurements of a sprite with halo event driven by a negative lightning discharge over Argentina, *Geophys. Res. Lett.*, *35*, L14812, doi:10.1029/2008GL033984.

Teich, T. H. (1993), Emission spectroscopy of corona discharges, in *Non-Thermal Plasma Techniques for Pollution Control*, edited by B. M. Penetrante and S. E. Schultheis, *NATO ASI Ser., Ser. G*, *34*, 231–248.

Thomas, J. N., et al. (2008), Sprites and halos produced by positive and negative cloud-to-ground lightning over argentina and brazil: Overview of video images, ELF/VLF data, and meteorology, paper presented at National Radio Science Meeting, U. S. Natl. Comm., Int. Union of Radio Sci., Boulder, Colo., 3–6 Jan.

Vallance-Jones, A. V. (1974), *Aurora*, D. Reidel, Norwell. Mass.

Zabotin, N. A., and J. W. Wright (2001), Role of meteoric dust in sprite formation, *Geophys. Res. Lett.*, *28*(13), 2593–2596, doi:10.1029/2000GL012699.

A. B. Chen, R.-R. Hsu, and H.-T. Su, Department of Physics, National Cheng Kung University, Tainan 70101, Taiwan. (alfred@phys.ncku.edu.tw; rrhsu@phys.ncku.edu.tw; htsu@phys.ncku.edu.tw)

H. U. Frey and S. B. Mende, Space Sciences Laboratory, University of California, Berkeley, CA 94720, USA. (hfrey@ssl.berkeley.edu; mende@ssl.berkeley.edu)

L.-C. Lee, Institute of Space Science, National Central University, Jhongli 32001, Taiwan. (loulee@ncu.edu.tw)

N. Liu, Geospace Physics Laboratory, Department of Physics and Space Sciences, Florida Institute of Technology, Melbourne, FL 32901, USA. (nliu@fit.edu)

V. P. Pasko, Communications and Space Sciences Laboratory, Department of Electrical Engineering, Pennsylvania State University, University Park, PA 16802, USA. (vpasko@psu.edu)